Resonant magnetic x-ray-scattering studies of NpAs. I. Magnetic and lattice structure

S. Langridge and W. G. Stirling
Physics Department, School of Science and Engineering, Keele University, Keele, Staffordshire ST5 5 BG, United Kingdom

G. H. Lander and J. Rebizant
Joint Research Centre, European Commission, Institute for Transuranium Elements, Postfach 2340, D-76125 Karlsruhe, Germany

(Received 29 November 1993)

The magnetic x-ray scattering from a transuranium material, NpAs, has been measured. We report the intensity of the scattering as a function of photon energy in the range of the M_{IV} and M_V absorption edges (3.5 to 4 keV). Large enhancements are found at the M-edge binding energies, as is the case in uranium compounds. We have used the strong M_{IV} resonance (3.852 keV) to examine the magnetic struture of NpAs as a function of temperature. Differences between the phase diagram as studied previously by neutron diffraction and the present experiments may be ascribed to the near-surface sensitivity of x-ray scattering. In particular we observe some unusual "domain" effects that may be attributed to surface anisotropy. The higher resolution available in the x-ray experiments, as compared to the neutron experiments, has led to an understanding of the wave vector dependence as a function of temperature. We suggest that the change of the wave vector from its commensurate value of 1/4 (corresponding to a square wave 4+, 4− arrangement of magnetic moments) may be understood by introducing "defects" into the magnetic structure. We confirm the earlier work that showed the lattice initially distorted to tetragonal (from the NaCl fcc structure in the paramagnetic state) and reverted to cubic in the low-temperature triple-**q** antiferromagnetic phase.

I. INTRODUCTION

The cross section for nonresonant magnetic scattering of x rays is some six orders of magnitude less than the normal charge (Thomson) scattering.[1] However, with the high brilliance of modern synchrotron sources, an increasing number of observations of magnetic scattering have been made.[2] During systematic experiments on holmium metal, Gibbs *et al.* discovered[3] that a large enhancement of the magnetic signal occurred when the photon energy was tuned to an L-absorption edge. Hannon *et al.*[4] identified the resonances as originating from electric multipole resonances, which contribute to the magnetic scattering when the energy excites an electron into a shell containing spin-polarized states. The largest effects are seen when a strong dipole ($L=1$) resonance occurs. Unfortunately, the energies for dipole resonances of $3d$ or $4f$ elements do not lie in a convenient energy range for *scattering* experiments, but can, of course, be exploited in studies of the absorption phenomena,[5,6] which occur at a momentum transfer (Q) of zero. The relevant absorption edges for the actinide ($5f$) elements lie in an energy range 3.5–5 keV and are therefore suitable for scattering experiments. Soon after the understanding of the resonant effects, experiments were performed on antiferromagnetic (AF) UAs.[7]

A number of experiments have now been reported that exploit the resonant effects in examining, for example, the coherence length[8] and temperature dependence of the magnetic order[8,9] in uranium-based materials. In an earlier publication,[10] we examined the resonant effects in a series of U compounds such as UO_2, in which the electronic configuration is U^{4+} ($5f^2$), and USb, in which the configuration is thought to be predominantly trivalent U^{3+} ($5f^3$). We focused particularly on the branching ratio (BR), which is the ratio of the enhancement of the signal at the M_{IV} edge compared to that at the M_V edge.

A number of motivations exist for continuing these measurements in actinide materials and extending them to materials with transuranium ions. (a) What can be learned about the magnetic structure of a system as complicated as NpAs? (b) Do the branching ratios vary in the way anticipated from theory as transuranium materials are examined? (c) Is it possible at resonance energies to see weak scattering from the spatial correlations in the critical regime, and how do the parameters extracted compare with those measured by neutron diffraction? (d) Given that it is difficult to produce and work with the large (>5 mm^3) samples containing transuranium elements (often necessary for neutron-scattering experiments) and quite impossible for elements beyond curium, do the new synchrotron sources present the possibility of exploring the microscopic magnetic properties of the heavier actinides and their compounds?

We describe the experimental arrangement in Sec. II. The measurements as a function of energy and the determination of the branching ratios are given in Sec. III. In Sec. IV we discuss the magnetic structure of NpAs and our study of this using x rays at the resonant energy. In Sec. V we present studies of the lattice behavior as a function of temperature using a high-resolution configuration. The discussion is given in Sec. VI. In the following paper

(II of the present series), we will discuss the results of the experiments performed on NpAs in the critical regime (i.e., near T_N). A preliminary account of this latter work has been published elsewhere.[11]

II. EXPERIMENTAL DETAILS

All the experiments described here were performed at the X22C beam line of the National Synchrotron Light Source (NSLS) at Brookhaven National Laboratory, and the method was identical to that described in our earlier work.[9,10] The beam line, which views synchrotron light from a bending magnet located in the 2.5-GeV NSLS storage ring, contains a doubly focusing nickel mirror and a fixed-exit Ge(111) double-crystal monochromator. Three Be windows are in the beam line, which together with the cryostat and sample holder give a total Be thickness of 1.7 mm. The energy and exit beam paths of the diffractometer were evacuated to minimize the absorption through air. Kapton windows are used for sealing these chambers; the total thickness of kapton in the beam was 0.28 mm.

The instrumental resolution at 3852 eV with respect to the (HKL) crystal coordinate system and described as the half-width at half maximum (HWHM) was measured at (002) as $\Delta q_L^R = 0.0018$ reciprocal lattice units (rlu), $\Delta q_K^R = 0.001\,15$ rlu, and $\Delta q_H^R = 0.0075$ rlu (1 rlu $= 2\pi/a = 1.076$ Å^{-1}). In this notation, Δq_L^R corresponds to the θ-2θ resolution, Δq_K^R to the θ resolution, dominated by the sample mosaic (which was 0.05°), and Δq_H^R to the resolution in the direction perpendicular to the scattering plane. The resolution function was determined by examining the chemical Bragg reflections, which could be adequately described by Gaussians. Since the observed magnetic peaks are frequently wider than the experimental resolution, we derive a coherence length ζ in real space by the relationship $\zeta = 1/\Delta q$, where Δq is in Å^{-1}. Note that for the high-resolution measurements of the lattice parameter discussed in Sec. V of this paper a different energy and diffractometer configuration were used; the resolution in this case is described in Sec. V.

The sample was a single crystal grown[12] at the Institute for Transuranium Elements, Karlsruhe, and measuring $\sim 2\times 2\times 0.3$ mm^3 (weight 12 mg). It was handled in a glove box and encapsulated in a special copper holder with a thin (0.2 mm) Be window, through which the x-ray beam passed, recessed into the capsule. The holders were placed in a standard closed-cycle cryostat so that temperatures down to ~ 12 K could be reached. The crystals have (001) cleavage planes, so that it is relatively straightforward to find ($00L$)-type reflections. Integrated intensities were always obtained by rocking the crystal through the Bragg condition for a given energy. Away from the resonance energies, the intensities are small and the background corrections from the fluorescence are large, thus causing scatter in the data points. Temperatures were determined by calibrated sensors in the copper block behind the sample. Self-heating effects due to radioactive decay in Np are negligible, but the absence of heat shields in the cryostat (to reduce the absorption of the x-ray beam) raises some doubts with respect to the absolute thermometry of this experiment.

III. MEASUREMENTS OF RESONANCES AND THE BRANCHING RATIO

Measurements were performed in the two commensurate phases of AF NpAs; a full description of the magnetic phase diagram is given in the following sections. In the type-I phase ($T < 130$ K) we measured the (001) reflection, and in the 4+,4− phase ($140 < T < 160$) we measured the (0,0,1.75) reflection. No difference was found between the energy dependence of the scattering of these two reflections. The results are shown in Fig. 1. We include also in this figure the results from a single crystal of USb, as determined in the study by Tang *et al.*[10] Note that the intensities are on a logarithmic scale.

The change in resonant energy going from U to Np represents the increase in binding energy for the increased nuclear charge and agrees with values extrapolated from tabulated values. It presents the possibility of determining whether each species carries a magnetic moment in scattering experiments on random magnetic alloys of actinides; this is not possible with neutron diffraction.

Hannon *et al.*[4] provided the theoretical basis for understanding the substantial enhancement of the magnetic scattering by introducing into the expression for the x-ray cross section the additional term

$$F_{LM}(E) = \sum_{ab} \frac{P_a P_{a(b)} \Gamma_x(aMb;EL)}{2(E_a - E_b - E) - i\Gamma} \tag{1}$$

for an electric 2^L multiple resonance (EL), where $|a\rangle$ and

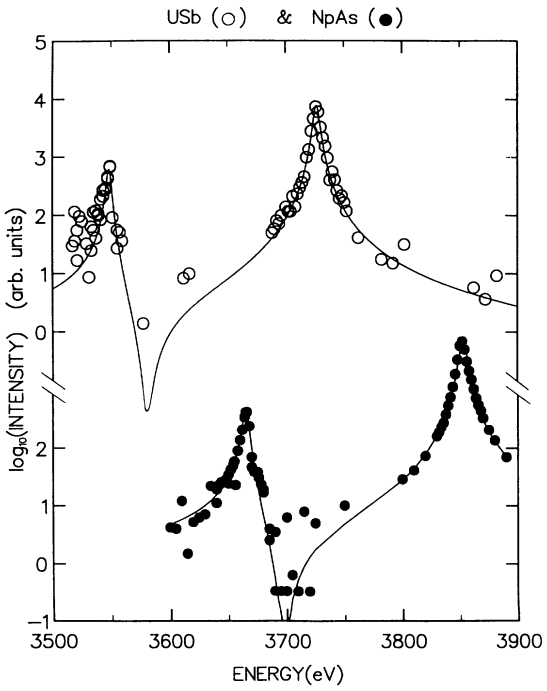

FIG. 1. Intensity of the scattered x-ray intensity from single crystals of USb (open circles, upper) and NpAs (solid circles, lower) as a function of the photon energy. The solid lines are fits described in the text.

$|b\rangle$ are the initial and final states of energy E_a and E_b, respectively, P_a gives the statistical probability for the initial state $|a\rangle$, and $P_a(b)$ gives the probability that the excited state $|b\rangle$ is vacant for transitions from $|a\rangle$. Summing over M, Γ_x gives the partial width for EL radiative decay from $|b\rangle$ to $|a\rangle$, and Γ is the total width for b. This term allows for the EL resonances to contribute to the magnetic scattering when the energy is such as to excite an electron into a shell which contains spin-polarized states. $F_{LM}(E)$ has maxima when $E=E_a-E_b$ and gives a Lorentzian form for the cross section. It may also contain more than one resonance contribution, and the resulting terms may interfere with one another.[7,10] The final cross section[4] for dipole scattering also contains the geometric term $(\boldsymbol{\varepsilon}\times\boldsymbol{\varepsilon}')\cdot\boldsymbol{\mu}$, where $\boldsymbol{\varepsilon}$ and $\boldsymbol{\varepsilon}'$ are unit polarization vectors of the incident and scattered radiation, respectively, and $\boldsymbol{\mu}$ is a unit vector in the direction of the magnetic moment. For the incident radiation polarized perpendicular to the scattering plane, the dipole term rotates the magnetic scattering σ to π and the geometric term reduces to $\boldsymbol{\mu}\cdot\mathbf{k}'$ in the amplitude, where $\mathbf{k}'$ is the wave vector of the outgoing beam. If the moment is perpendicular to the scattering plane, no resonant magnetic scattering will be observed.

The solid lines in Fig. 1 are fits to a theoretical function[10] based on two Lorentzians centered at the binding energies of the M_{IV} and M_V edges. Clearly, the two-resonance dipole model works well for both compounds, as found earlier in UAs (Ref. 7) and other U compounds.[10] The parameters in the fits are the resonant energies E, the full width at half maximum (FWHM) values of the Lorentzians Γ, and the amplitudes A. The positions E_4 and E_5 of the neptunium M_{IV} and M_V resonances are $E_4=3852$ eV and $E_5=3666$ eV with uncertainties of about 5 eV. The widths Γ are close ($\sim$6 eV) to the experimental resolution and essentially the same for both USb and NpAs. To allow an examination of lifetime effects in the resonant process requires energy resolution better than currently available on the X22C beam line.

Fitting to give the amplitudes A_4 and A_5 allows us to determine the branching ration ($BR=A_4/A_5$). Before discussing this in detail, we should like to briefly draw attention to the difficult experimental problem of treating absorption. Photons of this energy (3.5–4.0 keV) are strongly absorbed. The energy dependence of the Be, kapton, and air absorption in the beam is known and can be corrected for accurately. Much more difficult is the intrinsic absorption of the sample itself near the resonance, where it becomes strongly dependent on energy.[13] We have discussed this in detail in our earlier work.[10] The absorption curves used for U and Np are shown in Fig. 2. They have maxima near the resonant energies, and the experimental intensities must be corrected for this effect. In the absence of a direct measurement of the absorption, preferably in the same material as used for the scattering experiments, our conclusions must therefore remain qualitative. We note, however, that we derived the absorption corrections consistently[10] and that, in the case of the uranium material, they are based on the total electron yields of Kalkowski *et al.*[14] We have assumed that the white line absorption for Np behaves in an identical way to that for U, except that it is shifted to the corresponding binding energies. Tabulated values have been used for the regions between the absorption edges. We cannot do better than this until either appropriate absorption measurements are performed or relevant calculations are published.

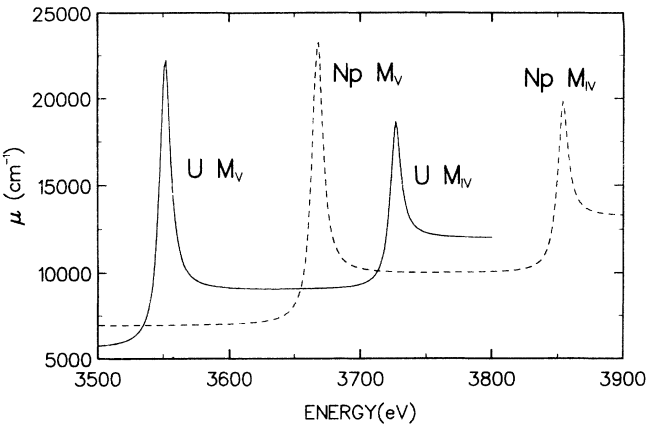

FIG. 2. Derived absorption coefficients (see text) as a function of photon energy for U and Np. The relevant absorption edges are identified.

The uncorrected values (i.e., no allowance for the energy dependence of the absorption corrections) for the branching ratios are, for USb, 5.1(2) (Ref. 10) and, for NpAs, 4.1(2). The corrected values are, for USb, 3.5(3) (Ref. 10) and, for NpAs, 3.0(3). The theoretical value for USb, derived[10] on the assumption of a f^3 (U^{3+}) configuration, is $\sim$6, whereas calculations[15] for Np^{3+} give $\sim$4, and so the experimental values appear somewhat smaller. These differences are not totally understood at this time, but the trend of a decreasing BR as we proceed from U to Np seems similar for both theory and experiment.

IV. MAGNETIC STRUCTURE OF NpAs

A. Previous work

The first study of the magnetic phase diagram of NpAs was reported 20 years ago by Aldred *et al.*[16] working with polycrystalline samples. The material is fcc (NaCl structure) with a lattice parameter of 5.838 Å at 300 K. Because of the series of interesting phase transitions discovered in NpAs, once single crystals could be produced,[12] a number of investigations were undertaken. Burlet *et al.*[17] examined the phase diagram in applied magnetic fields. Jones *et al.*[18] made a more thorough investigation of the ordering wave vectors and their temperature variation than had been possible with polycrystalline materials and followed this with experiments on the critical regime.[19]

We start (Fig. 3) with the overall magnetic phase diagram adapted from Jones *et al.*[18] Recall that we shall not discuss the critical regime near T_N in this paper; that is the subject of the following paper. From the neutron experiments, the material orders antiferromagnetically at $T_N\sim173$ K with an incommensurate longitudinal modu-

lation that has a wave vector of 0.233 rlu. This implies that the repeat distance in real space is $\Lambda = 1/0.233 \sim 4.29$ unit cells. By applying a magnetic field to the sample, Burlet *et al.*[17] showed that the structure is of the single-**q** type. This means that at high temperatures ($T > 140$ K) the crystal consists of three domains, each with a magnetic modulation propagating in one of the three equivalent ⟨001⟩ directions. In each domain the magnetic moments are parallel to the direction of propagation. Such a single-q-type structure is also consistent with the appearance of a tetragonal distortion of the unit cell just below T_N, as observed by Aldred *et al.*[16] In this tetragonal phase, the c axis is smaller than the a parameter, where c is defined as the propagation direction of the magnetic modulation. The magnetoelastic effects increase the spacing between atoms in the (001) ferromagnetic planes as compared to the spacing between the planes.

On further cooling, Jones *et al.*[18] observed a gradual change in the magnitude of the q vector until a lock-in transition to the commensurate value of $q = \frac{1}{4}$ (0.250) occurred at $T_{IC} \sim 158$ K. As shown in Fig. 3, the change of the q vector is also accompanied by the growth of the third-order harmonic, so that by the time the commensurate value of $\frac{1}{4}$ is attained the wave form is almost a square wave of the form $++++----$ or $4+,4-$, where each $+$ or $-$ represents a ferromagnetic (001) sheet of Np moments with the moment direction perpendicular to the magnetic sheet. For a perfect square wave in the $4+,4-$ structure, the ratio of the squares of the structure factors of the third- to the first-order harmonics is $(F_3/F_1)^2 = 0.17$. This model was further refined in subsequent work by Jones *et al.*,[19] in which they succeeded in measuring the weak fifth-order harmonic in the incommensurate state. The structure remains commensurate single **q** from T_{IC} until $T_0 \sim 140$ K, at which temperature a first-order transition occurs to a type-I structure with a simple $+-+-$ ($q = 1.0$) modulation. No further change in the magnetic structure occurs down to 2 K. The T_0 transition (there is considerable hysteresis in this transition depending on the thermal history of the sample) is of interest as, on cooling, a large increase occurs in the resistivity,[16,20] giving rise to speculation that the material undergoes either a valence change or a Mott transition to an insulating state. Below T_0, Aldred *et al.*[16] also reported that the material was *cubic*, i.e., that below T_0 it reverted to the cubic symmetry found in the paramagnetic state (after becoming tetragonal in the temperature range between T_N and T_0) and that the volume expanded by 0.25%. The cubic symmetry in the low-temperature state is now understood on the basis that the magnetic structure below T_0 is actually of the triple-**q** type, in which the three components of the modulation exist *simultaneously* in one domain. Since the 3-**q** structure has cubic symmetry (the resultant moment direction in the 3-**q** state is along one of the ⟨111⟩ axes), this explains why the unit cell reverts to cubic below T_0. The 3-**q** structure is common in actinide compounds with the NaCl structure (see, for example, Rossat-Mignod, Lander, and Burlet[21]), although it is unusual to observe a transition from triple **q** to single **q** as a function of temperature.

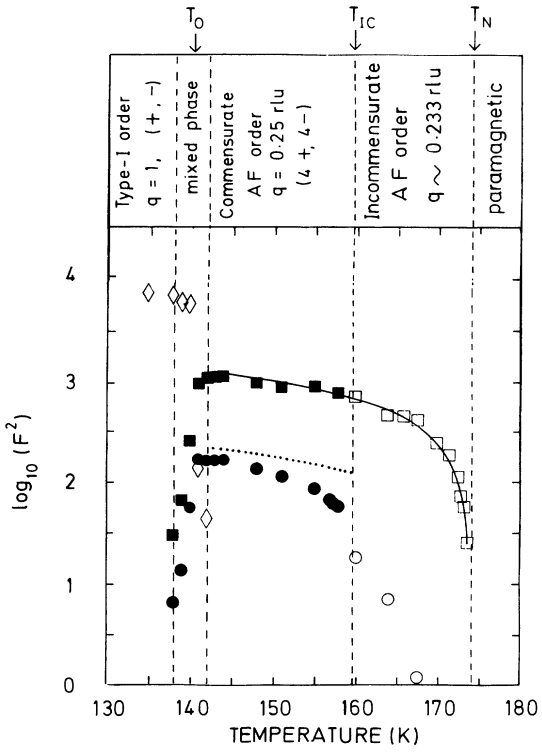

FIG. 3. Details of the magnetic phase diagram as a function of temperature as determined by neutron diffraction and reported by Jones *et al.* (Ref. 18). The ordinate axis is the square of the structure factor, which is directly proportional to the intensity; note the logarithmic scale. Squares, first-order harmonics; circles, third-order harmonics; diamonds, $q = 1$ modulation below T_0. The solid line through the first-order harmonics is a fit to the neutron data with a β parameter $= 0.38(1)$. The dashed line in the commensurate phase corresponds to the predicted intensity of the third-order harmonic if a regular square-wave modulation exists. The magnetic moment at 10 K is $2.5(1)\mu_B$. There is a discontinuity in the value of the moment at T_0; above this temperature, the neutron experiments determine $\sim 1\mu_B$.

Although the temperatures of the phase transitions found by both Burlet *et al.*[17] and Jones *et al.*[18,19] were in good agreement with each other, as well as with the earlier work,[16] we have found some significant differences (as much as 10 K in the case of T_0) in the present x-ray experiments. We have already discussed some possible problems with our thermometry in the x-ray experiment in Sec. II, and to these must be added the possibility that the x-ray experiments are sensitive to the near-surface behavior of the material (see below). However, all experiments have found the same sequence of phase transitions, and we do not attach any significance to the differences in temperature.

B. Geometrical considerations for the x-ray experiments

We have already seen in Fig. 2 that the absorption of x rays at the M_{IV} resonance ($E = 3852$ eV, $\lambda = 3.219$ Å) is large, $\mu \sim 2 \times 10^4$ cm^{-1}. This means that the penetration

of the x rays is small. For example, at a Bragg angle of 30° the $1/e$ penetration depth is only 1200 Å (recognizing that the beam must also come out of the sample). Experiments at these energies are therefore sensitive to the near-surface magnetic structure, whereas the neutrons are a true bulk probe.

Figure 4 shows in (a) the portion of reciprocal space covered by the present experiments (all scans are either along the L or K axes) and in (b) a schematic drawing of crystal blocks in real space. Each of the three domain types A, B, and C will scatter radiation into different parts of reciprocal space, due to the translational symmetry of the magnetic structure. Our experiments sample the L line between (001) and (003) and the K line between (002) and (012). Domains of the type C are sampled along L and those of type B along K. Our experimental geometry is such that the resolution along H is too poor

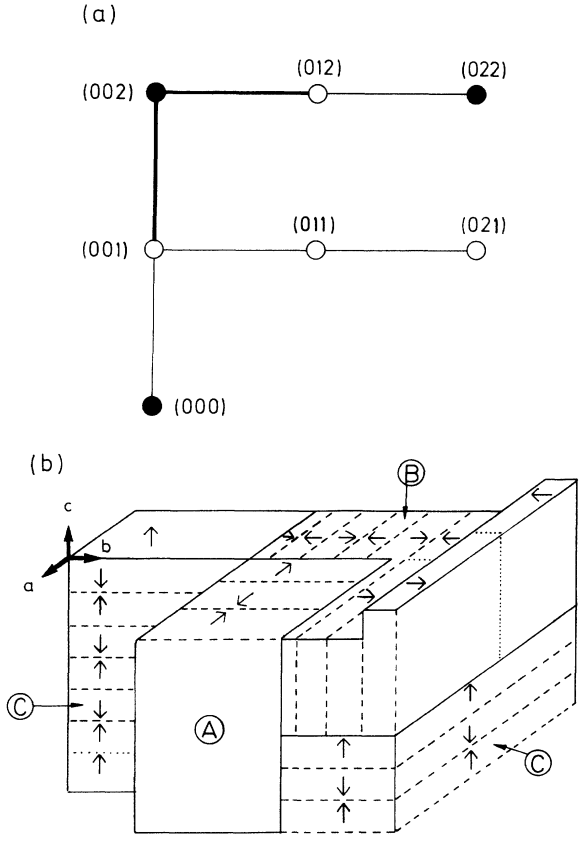

FIG. 4. (a) Reciprocal space examined in the present x-ray experiments. Scans were made in the direction (002)→(012), a K scan, and (001)→(002), an L scan. (b) Schematic drawing of the crystal showing the different types of magnetic domains. Each arrow represents four magnetic moments (i.e., two unit cells). In the high-temperature phase, the scattering from the C domains (with moments parallel to c, $\mu \| c$) will occur along the L line in reciprocal space, whereas scattering from B domains ($\mu \| b$) will occur along the K lines in reciprocal space. A domains ($\mu \| a$) with scattering along the H axis are not observed with the scattering geometry of the present experiments. Solid lines represent domain boundaries, dashed lines are changes of moment direction within one domain, and the dotted lines are other possible antiphase domain boundaries.

for it to be useful to examine domains of the A type. Since our experiments are sensitive to the near-surface magnetic structure, we note that there is a difference between domains C on the one hand, and A and B on the other. The C-type domains have their moments normal to the surface, whereas the A- and B-type domains have their moments lying parallel to the surface [see Fig. 4(b)]. It will be important to bear these geometrical considerations in mind when we examine the details of the domain structure as a function of temperature. Of course, below T_0 in the type-I phase, the domain structure of Fig. 4(b) does not apply, since the magnetic structure is of the 3-q type (see above).

A further factor is that arising from the term $\mu \cdot \mathbf{k}'$ in the resonant cross section, as discussed in Sec. III above. For the $(00L)$ magnetic reflections near (002), the angle between the outgoing x-ray beam ($\mathbf{k}'$) and the moments, which are perpendicular to the surface [see domains C in Fig. 4(b)], is ~60°, so that the geometrical factor modifying the scattering intensity is ~0.25. On the other hand, for the B domains in Fig. 4(b) the outgoing wave is only some 12°–20° from the moment direction, so that the factor is close to 0.9. This means that if the domains are equally populated we anticipate the $(0K2)$ reflections to be about a factor of 3– to 4 more intense than the $(00L)$ type.

C. Results for first-order harmonic

As a prelude to the discussion of the detailed experiments, we show a complete scan in the commensurate phase along the L axis from $L=1$ to 3 in Fig. 5. This figure shows the considerable intensity in the first-order harmonics at $L=1.75$ and 2.25 corresponding to over 2×10^4 counts per second.[22] The third-order harmonics are readily observed at $L=1.25$ and 2.75. Additional spurious peaks arise from $\lambda/3$ components (at $L=\frac{4}{3}$ and $\frac{8}{3}$ and from scattering by the sample cell. These spurious peaks may be identified, as their intensities do not change

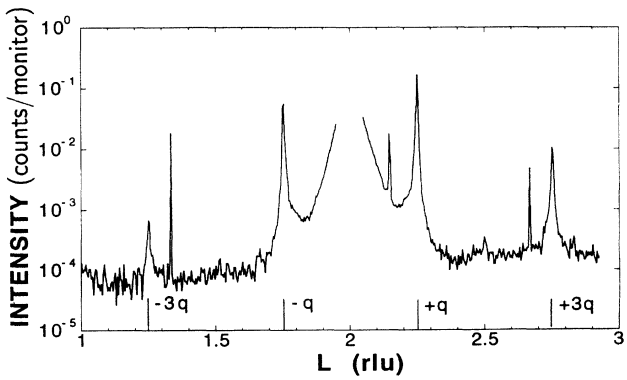

FIG. 5. X-ray scan ($E=3852$ eV) along the L direction in reciprocal space at $T=135$ K in the 4+,4− phase showing first- and third-order magnetic peaks. The large peak at $L=2$ is the charge peak. Other contributions come from higher-order contamination (at $L=\frac{4}{3}$ and $\frac{8}{3}$) or spurious processes and are independent of temperature.

either with temperature or energy.

As a useful digression here, we point out that in a comparable neutron experiment on a material with this type of magnetic structure there will be *no* magnetic scattering along the $(00L)$ line in reciprocal space. This is because the magnetic interaction vector and the moments in the C domains are parallel to Q for the $(00L)$ reflections. The conditions are different (and more complex) in x-ray magnetic scattering.

The intensities of the first-order harmonics as determined by x rays in the L and K directions are shown in Fig. 6(a). An analysis of the intensities near T_N will appear in the following paper. We see from Fig. 6(a) that the B domains are preferentially populated at all temperatures between T_N and 138 K. A more direct illustration of this effect is provided in Fig. 6(b) where we present the ratio of the volumes of the C domains to the total volume as a function of temperature. Figure 6(b) is derived on the reasonable assumption that domains A and B are equally populated.

At a temperature of 138 K, there is a sudden enormous increase in the population of the C domains and a corresponding reduction of the intensity from the B domains, so that for a small range of temperature just above T_0 (130 K as measured in these experiments) the near-surface region consists almost completely of C domains. It is difficult to understand the reason for this abrupt domain reorientation just above T_0; one possible origin is in magnetoelastic effects. The tetragonal distortion[16] appears at T_N and gradually increases down to T_0. The domain reorientation appears to be a *precursor* of the transition from a single-q to a triple-q structure, which is surprising since this transition is clearly of first order. We have not been able to find any unusual effects connected with the lattice behavior at this temperature; see Sec. V. These domain effects are not observed in the neutron experiments; the antiferromagnetic domain populations throughout the bulk are always equal, i.e., 33% of the volume in each domain.[17–19] Furthermore, at low temperature in the triple-q state the intensities of the (001) and (012) magnetic reflections are of comparable magnitude. This is anticipated because for each reflection the intensity in the triple-q state comes from the total illuminated volume.

We turn now to the values of the modulation wave vectors observed by scans in the L direction near (0,0,2.2) and in the K direction near (0,0.2,2). These are shown in Fig. 7. The first point to note is that the values of q are *different* for the two domains at high temperature near T_N. These differences are outside the standard deviations, which are approximately the size of the data points, especially below 170 K, when the reflections are intense [see Fig. 6(a)]. Based on our determination of the

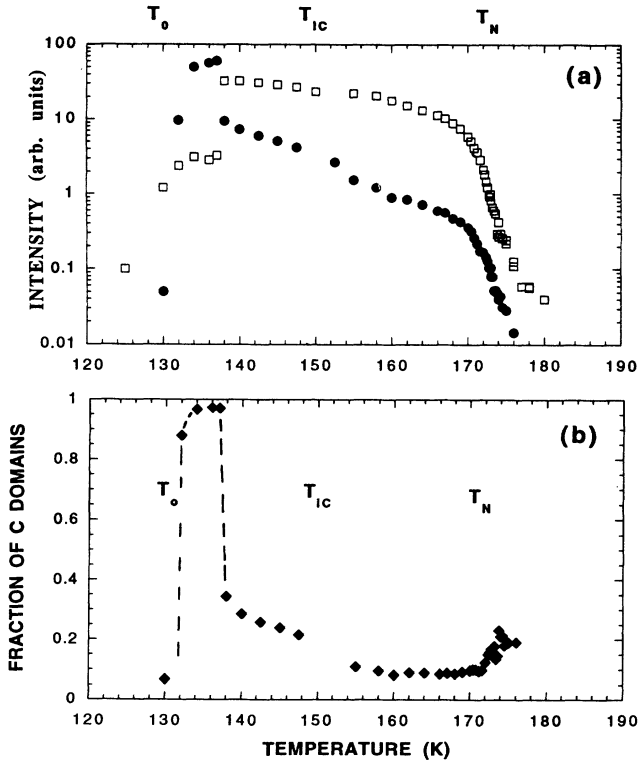

FIG. 6. (a) Intensity (on a logarithmic scale) of the first-order harmonics in the L (solid circles) and K (open squares) directions corresponding to C and B domains, respectively, as measured by x rays. (b) Calculated "C-domain fraction" based on the assumption that A and B domains are equally populated.

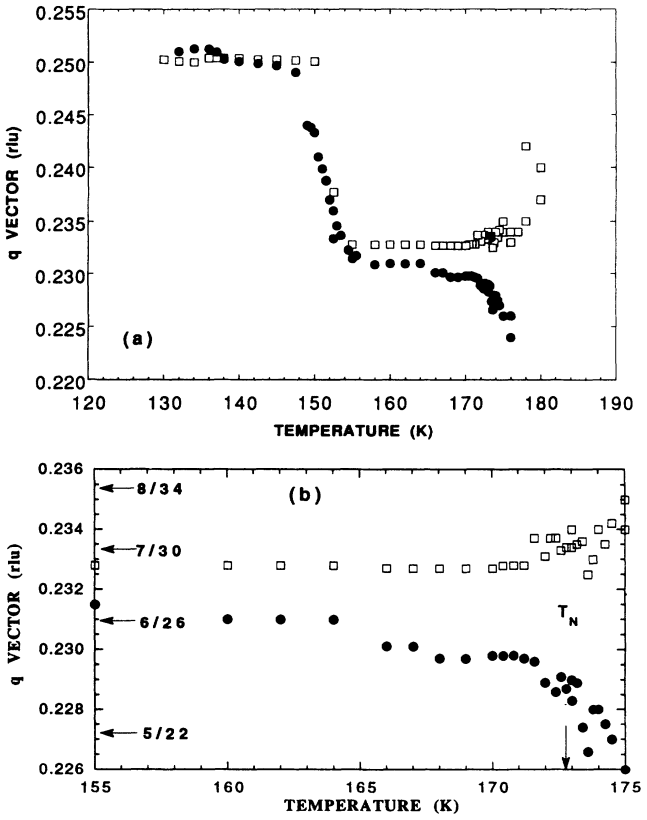

FIG. 7. (a) q_L (q_K) values for the C (B) domain shown as solid (open) symbols. The q_L values appear to differ from $q = \frac{1}{4}$ at low temperature because of the tetragonal lattice distortion. (b) Details of the modulation wave vectors near T_N. Different possible commensurate values of the wave vector and T_N are marked.

position of the lattice points, e.g., (002), we estimate a precision of ± 0.0005 rlu. Some further uncertainty arises because of the lattice distortion (see Sec. V), and this distortion is responsible for the C-domain q values appearing slightly different from the commensurate value of 0.250 rlu below T_{IC}. The mean values between 155 and 170 K are $\langle q_L \rangle = 0.2305(5)$ rlu and $\langle q_K \rangle = 0.2330(3)$ rlu. Since the wave vectors remain constant over this temperature range, it is tempting to speculate that they may correspond to some commensurate values. The commensurate value close to $\langle q_L \rangle$ is $\frac{3}{13} = 0.2308$ and to $\langle q_K \rangle$ is $\frac{7}{30} = 0.2333$. Recall that these modulation wave vectors (q_K and q_L) come from *different* volumes of the crystal. A further discussion is given below in Sec. IV E.

We have examined also the widths of the reflections, both in the directions parallel and perpendicular to the magnetic propagation direction. For the temperature ranges $139 < T < 148$ K and $155 < T < 170$ K, the q_K peaks are almost resolution limited in both directions, consistent with a large population of B domains [see Fig. 6(a)]. The q_L peaks, on the other hand, are wider ($\Delta q_L = 0.0030$ rlu) than the resolution function (0.0018 rlu) in both the longitudinal and transverse directions throughout this temperature range, suggesting that the coherence length of the C domains is only ~ 400 Å. Exactly the reverse situation is observed below the reorientation transition shown in Fig. 6(b). In the range $131 < T < 138$ K, the q_L peaks now become resolution limited, whereas the q_K peaks show significant broadening. We defer a discussion of the intermediate range $148 < T < 155$ K until Sec. IV E.

For temperatures below T_0 in the type-I phase, the magnetic scattering occurs at the (001) and (012) positions. Significant broadening of the peaks was observed in this phase and is caused by the lattice distortion; see Sec. V.

D. Results for higher-order harmonics

The greater intensity observed in the x-ray experiments, compared to the neutron experiments, led to an anticipation that a more complete study could be made with x rays of the higher-order harmonics. The neutron results[18] (Fig. 3) show that the ratio of the intensity of the third- to first-order harmonic intensities is close to that for a square wave (17%) below T_{IC} and that even near T_{IC} this value is still $\sim 3\%$. Moreover, Jones *et al.*[19] showed that it was possible in neutron experiments to observe the fifth-order harmonic in the incommensurate state (in the $q = \frac{1}{4}$ state the first- and fifth-order harmonics occur at the same position); the fifth-order harmonic reached a maximum intensity just above T_{IC} of 0.5% of the first-order harmonic. In the case of both neutron and nonresonant magnetic x-ray scattering, the cross sections from the different components of a modulated structure are well understood, and the above ratios are based on these expectations. However, it is not immediately clear that this is also the case in the case of *resonant* x-ray scattering. Based on the results presented here and in Ref. 9, it does appear that the Fourier harmonics may be factored out of the cross section, but although additional theoretical details of the cross section have been presented recently,[23] this point has not been addressed explicitly.

The ratios of the intensities of the third- to first-order harmonics observed with x rays and neutrons are shown in Fig. 8. The ratio of the fifth- to first-order harmonics in the neutron case is shown by the solid line. Concentrating initially on the x-ray results, we see a significant difference between the results for the B (open squares) and C (open circles) domains. Below $T = 138$ K, the magnetic structure in the C domains is essentially a square-wave modulation, and the widths of both the first- and third-order harmonics are close to the resolution limit. The third-order harmonic from the C domains could not be observed for $T > 138$ K. We recall that in this temperature range the C domains have a small population [Fig. 6(b)] and relatively short coherence length as defined by the first-order harmonics, so that the difficulty in observing the higher-order harmonics of the C domains is not surprising.

However, it is surprising that it is so difficult to observe the higher-order harmonics of the B domains in the temperature range $T > 138$ K over which they dominate. This is particularly so because the widths Δq_K of the first-order harmonics become resolution limited below T_N. The third-order harmonic is weak and has a width suggesting a coherence length for this modulation of ~ 200 Å. No fifth-order harmonic could be observed. To our knowledge this is the first example in which magnetic AF domains with their propagation vectors lying in and normal to the surface have been examined by a surface-sensitive diffraction technique, and it will be interesting to extend these types of measurements to other systems.

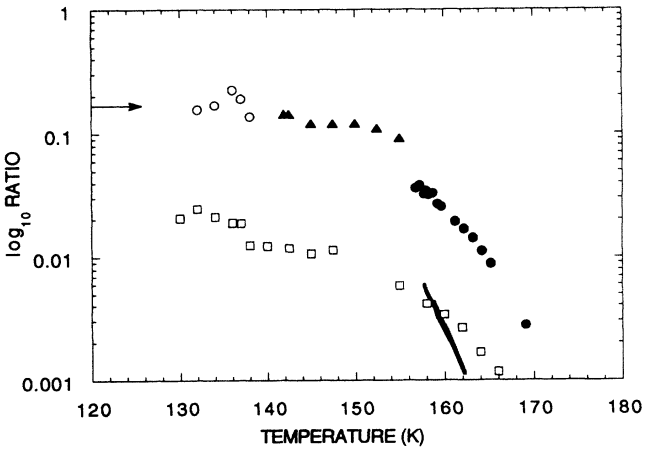

FIG. 8. Ratio of the squares of the higher-order structure factors to that of the first order in NpAs. Open circles (squares) correspond to the ratio third/first for x rays from the C (B) domains. Solid circles (triangles) correspond to the results from the neutron experiments in the commensurate $q = \frac{1}{4}$ (incommensurate $q < \frac{1}{4}$) regions. For a completely squared modulation in the $q = \frac{1}{4}$ commensurate state, the theoretical value of this ratio is 0.1716, which is marked with an arrow on the ordinate axis. The solid line corresponds to the ratio of fifth- to first-order harmonics as measured in the neutron experiments (Refs. 18 and 19).

The differences between the neutron and x-ray results as shown in Fig. 8 are considerable; similar differences have been found in other systems.[9,24]

E. Models for the T dependence of the wave vector

One of the most interesting aspects of this study is the observation of the temperature dependence of the wave vector for the region ($148 < T < 155$ K) just before q attains the value of $\frac{1}{4}$. This is a complicated region since *both* commensurate and incommensurate peaks exist simultaneously. We demonstrate this in Fig. 9. In Fig. 9(a), corresponding to an examination of the C domain wave vector, q_L changes from 0.233 rlu at 153 K to 0.250 rlu at 148 K. At intermediate temperatures more than one peak is seen, and those at wave vectors between the two extreme values exhibit considerable broadening. The situation at 152.5 K for the B domains is shown in Fig. 9(b). Here there are two *sharp* peaks at the extreme values and, in addition, a *broad* peak at an intermediate value of q_K. The sharp peaks in Fig. 9(b) imply that these values correspond to *commensurate* values of q_K, and this is consistent with the fact that the q vectors are independent of temperature (Fig. 7) over the range $\sim 155 < T < 170$ K. Interestingly, a close examination of the q values as measured by neutron diffraction suggests that they also are independent of temperature just below T_N and then change to $q = 0.25$ rlu over a narrow temperature interval. In this respect the near-surface and bulk properties appear to be similar.

Figure 10(a) shows the wave vector widths (suitably deconvoluted with the resolution function) along the $(00L)$ line for the data of Fig. 9(a). To perform this analysis, we have assumed that the scattering centered at the two extreme values of q (0.2308 and 0.25) is resolution limits. Figure 7(a) suggests that the process of changing wave vectors is continuous. The widths Δq_L [Fig. 10(a)] are not resolution limited at high temperature. On cooling, the width increases on entering the intermediate region and then rapidly drops to the resolution function as soon as the wave vector becomes commensurate with $q = 0.25$ rlu. Figure 10(b) shows the widths of the first- and higher-order harmonics as measured by neutron

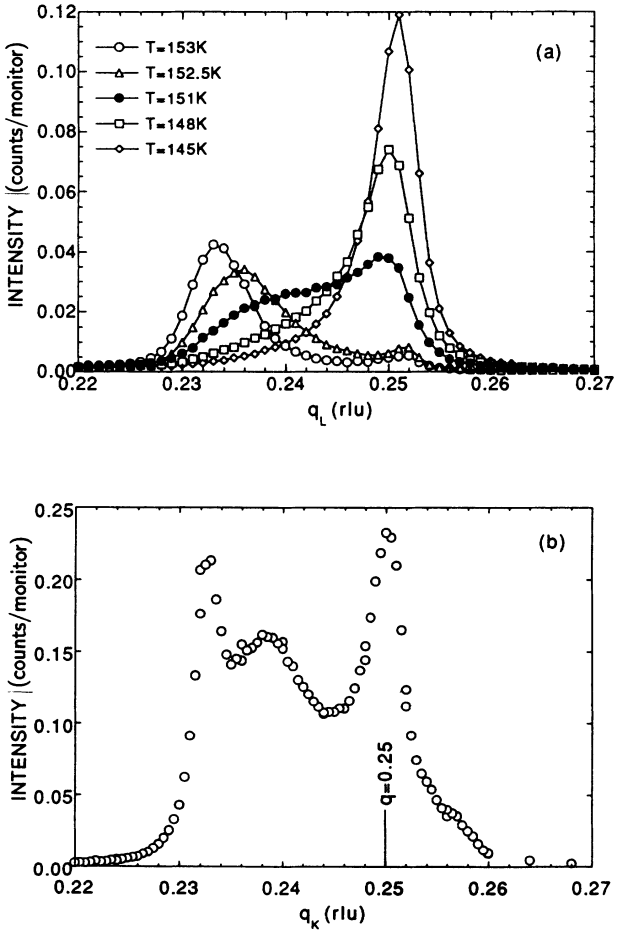

FIG. 9. (a) Experimental scans at different temperatures along the L axis showing the existence of both the commensurate and incommensurate phases in the temperature range $145 < T < 153$ K. The lines through the points are guides to the eye. (b) Similar scan in the $[0K2]$ direction at 152.5 K.

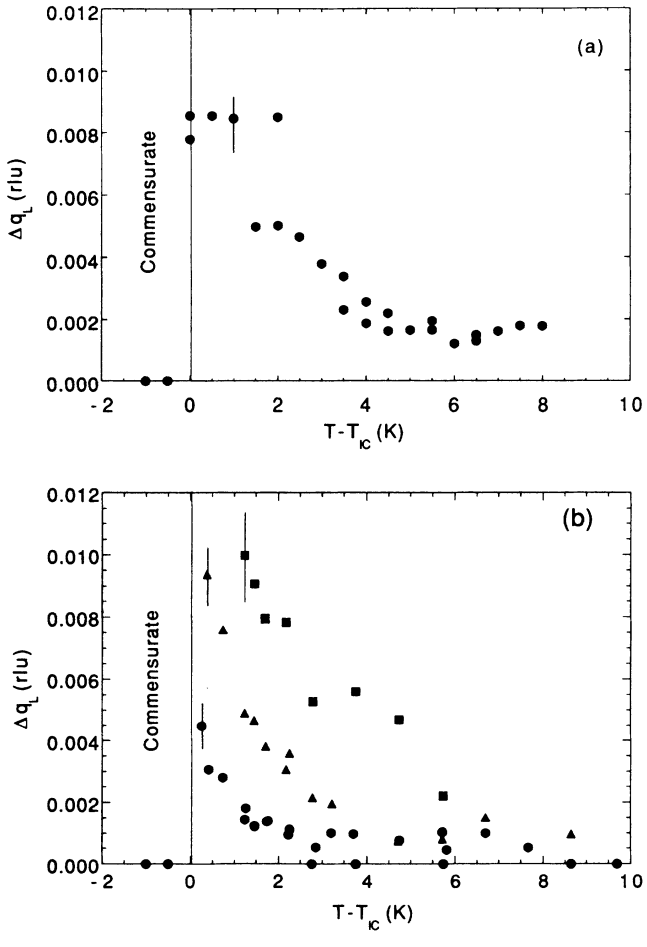

FIG. 10. (a) Deconvoluted widths (HWHM) as a function of temperature from the $[00L]$ scans. (b) Results from the neutron study of Jones *et al.* (Ref. 19) giving the deconvoluted widths of the various harmonics as a function of temperature near T_{IC}; the neutron resolution width (HWHM) was 0.005 rlu. First order satellites ●, third order ▲, fifth order ■.

diffraction.[19] Although the measured temperatures are different, as we have discussed before, there is a strong similarity between the behavior of the widths as measured in the two experiments over this temperature range.

We describe this process as one of changing between two commensurate values of the wave vector. Clearly, that at $q=0.25$ rlu is the simplest consisting of a $4+,4-$ configuration. On heating beyond T_{IC}, the wave vector *decreases* and there is a large increase in the widths. On further heating, q decreases and there is an accompanying decrease in the width until a new (more complicated) magnetic configuration is reached. At this temperature the widths are comparable to their values in the $4+,4-$ region. Moreover, the widths of the higher-order harmonics in the neutron experiments [Fig. 10(b)] show an even more pronounced temperature dependence of the widths. That this is observed in the neutron experiments shows that the process is a bulk effect.

A possible model recognizes that to destroy the regular $4+,4-$ arrangement it is sufficient to introduce "faults" into the system. The simplest such fault is a plane of five rather than four parallel spins. (Introducing a plane of three spins will result in the q vector becoming larger, not smaller.) Writing the regular structure of $4+,4-$ as $\langle 4 \rangle$, the fault model may be written as $\langle 4^n 5 \rangle$, representing n blocks of four spins followed by one fault of five spins. Recognizing that we must place as many $5+$ as $5-$ sequences to preserve the antiferromagnetism, the q vector becomes $q=(n+1)/(4n+5)$. The number of faults is proportional to $1/n$, e.g., for $q=\frac{1}{4}$ with no faults $n=\infty$. Interactions between the faults tend to make the fault spacings regular and so mitigate against $n=$odd in this model. The likely values are then $n=2$ ($q=\frac{3}{13}=0.2308$), $n=4$ ($q=\frac{5}{21}=0.2381$), etc. Already at $n=4$ there is a large distance between the faults, and so for even greater values of n it would seem likely that the fault distributions are not uniform. For example, a coexistence of domains with $n=4$, 6, and 8 would lead to a wide peak centered at $q\sim 0.241$. Since (in this model) the width of the peak reflects not only the spread of individual q values, but also the spatial extent of each domain, no simple model can be used unless a number of assumptions are made. Such ideas lead to the peak width being large for large n, a situation observed when the faults are initially introduced and consistent with the experimental observations shown in Fig. 10.

This model does not give a q value near $\frac{7}{30}$. However, it can easily be generalized with the formula $\langle 4^n 5^m \rangle$, so that $q=(n+m)/(4n+5m)$. The generalized model recognizes that faults may occur in pairs $(5+,5-)$, whereas the previous model assumes the faults occur singly ($m=1$). If $m=2$, the new repeat distances have $n=3$ ($q=\frac{5}{22}=0.2273$), $n=5$ ($q=\frac{7}{30}=0.2333$), etc. The observation of q close to $\frac{7}{30}$ might suggest that at reasonably low density (i.e., not $n=1$ or 3) the faults may occur in pairs.

The above discussion, leading as it does to the concept of a "devils staircase" of commensurate phases, is in many respects similar to the situation in the rare earths with spin-slip structures.[25] So far, little account of the *widths* of the reflections has been taken in models involving spin-slip structures, although very substantial changes in the peak widths were observed, for example, in the study on erbium. The difficulty in making the model quantitative is that we need some idea of *both* the fault distribution and the spatial coherence of a certain distribution. The first may be modeled, as shown by the work of Brown *et al.*[26] in connection with diffraction effects observed in Sr-doped La_2NiO_4. To investigate the spatial long-range coherence, we plan a study of the material PuBi (Ref. 27) with resonance magnetic scattering. This material has a $\langle 4^2 5 \rangle$ structure with $q=\frac{3}{13}$, and one measure of the long-range coherence will be whether a lattice modulation at $q_{\text{lattice}}=\frac{2}{13}$ also exists.

V. STUDIES OF THE LATTICE

To study the behavior of the lattice, we have used an x-ray energy of 8 keV and a Ge(111) analyzer. We performed both L and K scans through the (002) and (004) Bragg peaks as a function of temperature. (The magnetic peaks were not observed at this energy, which is far from the resonance.) The resolution widths (HWHM) in these scans were 0.0005 rlu at the (002) in both the L and K directions. The data are shown in Fig. 11. The lattice parameters may be deduced directly from these scans, the

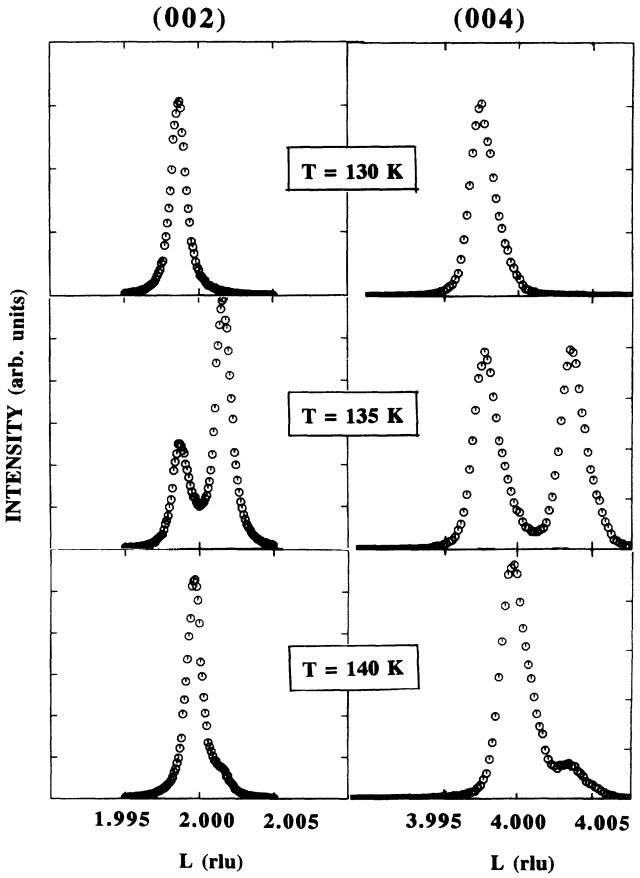

FIG. 11. Profiles of the (002) and (004) diffraction peaks taken with the high-resolution configuration (8 keV, Ge analyzer) at 130, 135, and 140 K.

separation of the two peaks being proportional to the tetragonal distortion. At 130 K (below T_0), only one peak is seen, confirming the results of Aldred *et al.*[16] that the material is *cubic* in the low-temperature triple-q state. The results given in Ref. 16 are reproduced in Figs. 12(a), and in 12(b) we compare them with the results deduced in the present experiment. For convenience we have normalized to the lattice parameter at T_0 in each case.

Because of the sensitivity to crystal alignment, the intensities in Fig. 11 are not necessarily reliable. Nevertheless, it is interesting to note that in the center panel ($T=135$ K), at which temperature the C domains dominate in the magnetic scattering, the contribution from the $(00L)$ planes is stronger than that from the $(H00)$ or $(0K0)$ planes.

The widths in the L direction of the (002) and (004) reflections in the triple-q state at low temperature are resolution limited. However, we have found that the transverse width (K scans) are broader. This corresponds to a change in the *mosaic* structure of the crystal. In fact, the crystal surface seems to distort to give two or more peaks of a total width corresponding to $\sim 6\times 10^{-4}$ rad. Since the transverse widths of the (004) are exactly a factor of 2 greater than those of the (002), we can be sure that it is the mosaic that is changing, presumably due to internal strains associated with the expansion in the volume at T_0. Similar "strain" effects to those reported here were seen by Knott *et al.*[28] using single crystals of uranium compounds that also have the triple-q AF magnetic structure. Our measurements are consistent also with the broadened powder diffraction profile observed in the original experiments by Aldred *et al.*[16] In the case of powder experiments, it is difficult to separate the effects of mosaic distribution, which in our present experiment affects the transverse widths, and strain in the lattice planes, which is observed as a broadening in the longitudinal direction.

We have also searched for lattice distortions associated with the $q=\frac{1}{4}$ magnetic structure at 137 K, when the C domains sustain a square-wave modulation. One might expect a second-order peak at the wave vector $q=\frac{1}{2}$ (as was found in UAs (Ref. 7)], but none was found in the present case.

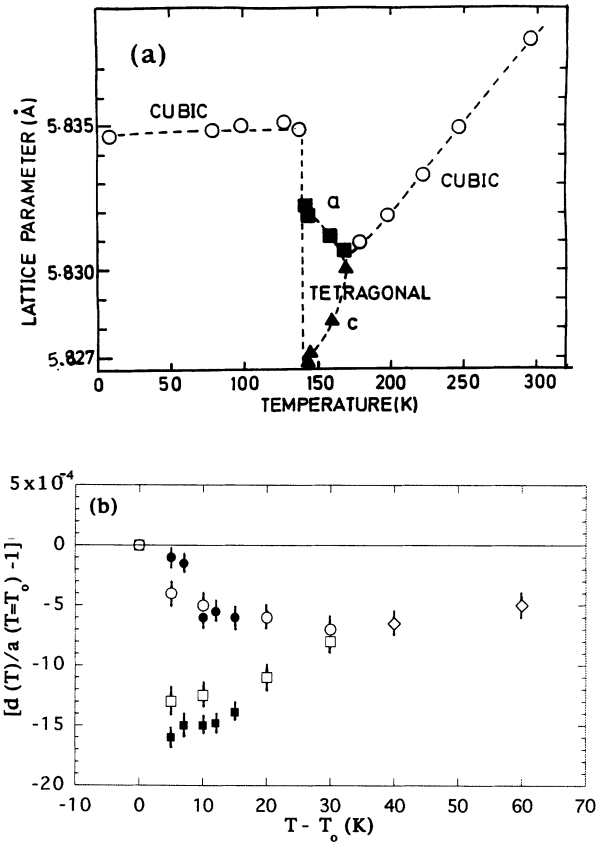

FIG. 12. (a) Lattice parameters as a function of temperature as reported by Aldred *et al.* (Ref. 16). (b) Relative lattice parameters, where d may represent the a or c lattice parameter (normalized to the cubic value of a at $T=T_0$), as measured in this experiment (solid symbols) and as determined by Aldred *et al.* (Ref. 16) (open symbols). The circles (squares) represent the a (c) lattice parameters in the tetragonal state. The lattice parameter in the paramagnetic state is represented by diamonds.

VI. DISCUSSION

The M_{IV} and M_V resonances in neptunium are as strong for resonant magnetic x-ray scattering as they are for uranium. The positions of the resonances are in good accord with extrapolations from the known resonances of Th and U. The branching ratio (ratio of M_{IV} amplitude compared to that at the M_V edge) is qualitatively consistent with the expectations of atomic physics calculations. Greater efforts will have to be made to account for the absorption on the experimental side before quantitative comparisons can be made.

The higher q-space resolution of the x-ray synchrotron diffractometers as compared to that available with neutrons has, indeed, allowed a more complete examination of the complex magnetic phase diagram of the actinide material NpAs. In particular, the variation of the q vector with temperature suggests that a situation analogous to the spin-slip structures of the rare-earth metals[25] occurs also in these actinide NaCl structure materials. The changing of the q vector introduces "faults" that repel each other once their concentration is sufficiently high, and this stabilizes more complex magnetic structures. An interesting intermediate region is observed as the structure first departs from the commensurate $4+,4-$ ($q=\frac{1}{4}$) arrangement, in which the widths of the diffraction peaks suddenly increase. A qualitative model has been proposed to explain these effects.

Some of the above ideas were already indicated by the neutron results,[16-19] and the synchrotron experiments have allowed more details to be extracted. What is quite new, however, is the suggestion from this experiment that the surface nature of the x-ray probe plays a major role. With a penetration of ~ 1200 Å, one might at first suppose that the major effects would be similar to the "bulk" of the material. This is not the case. Take the domain effects illustrated in Fig. 6 or the different q vectors at high temperature for the two domain states illustrated in

Fig. 7. These give a direct proof of the single-q nature of NpAs at high temperature. Normally, in neutron-diffraction experiments, the domain populations are observed to be equivalent, and the only way to decide whether the structure is single or triple q is to apply a symmetry-breaking perturbation such as a magnetic field[17] or uniaxial stress.[21] These synchrotron experiments show that the sample surface is indeed such a perturbation and that its influence extends quite far into the bulk. Since the present sample has not been prepared in any special way, we emphasize that the surface undoubtedly consists of an oxide overlayer and (probably) a high density of defects. Our present experiments are "near-surface" rather than "surface" sensitive. See Ref. 24 for a discussion of a similar problem.

At ~ 135 K we have observed a new kind of phase transition in which the domain populations change spontaneously as a precursor to the first-order phase transition in NpAs. Such reorientations might have a pronounced effect on properties such as the resistance, Hall effect, and magnetoresistance, measurements of which are normally performed on small thin samples. However, this "phase transition" is not seen in neutron diffraction as this technique samples the bulk of the material. The reorientational transition observed for the domains is probably related to magnetoelastic effects. We note that, in the ordered single-q state, the a lattice parameter is greater than c (see Fig. 12). If the surface region has predominant A and B domains, which minimize the dipole energy, the surface planes will tend to distort *monoclinically,* giving rise to additional strain components. When $(c-a)$ is small, the additional strain energy is negligible, but it increases as $|(c-a)|^2$, so that the preferred orientation is that where the moments lie perpendicular to the surface plane, giving rise to a sudden shift of the surface domains to be predominantly of the C type. If this is the mechanism driving the reorientational transition, it is noteworthy that it is a *surface* effect.

With respect to the magnetic modulation, the near-surface region also has different properties as compared to the bulk. In the bulk the neutron experiments show that the wave form is appreciably "squared" even in the incommensurate state. The fifth-order harmonic was, for example, observed by neutron diffraction. However, the near-surface region is quite different. Only a small amount of "squaring" is observed in all components until the reorientational transition takes place, when the magnetic modulation does indeed appear to develop its full squaring; see Fig. 8. Defects, steps, and roughness presumably play a role in limiting the coherence of the magnetic modulation, although whatever drives the reorientation ordering into C domains just above T_0 (and we have proposed that it is the competition between the dipole and strain energies) is also capable of setting up long-range order parallel to the surface normal in the near-surface region. Once the near-surface region has a C-domain orientation, there is no strain associated with domain boundaries between possible A and B domains, which have the same energy, so that truly long-range order is possible.

These "domain" effects constitute both an advantage and a hazard for x-ray experiments. The advantage is that we are clearly approaching the study of real "surface antiferromagnetism." If our interpretation is correct, the observation of the reduction in the C domains *above* T_N is, for example, the first observation in an antiferromagnet of the fact that the surface dipole energy[29] is sufficient to change the domain population of the near-surface region. At a surface of the C domain, the surface plane is, of course, ferromagnetic. We note that the magnetic anisotropy in these actinide systems is large, but in all A, B, and C domains the moments are aligned along a cube axis $\langle 100 \rangle$, so that anisotropy does not play a role in these discussions. The hazard, of course, lies in the necessity to be aware of these effects. If possible, it is clearly a great advantage to perform *both* neutron and x-ray experiments.

Finally, we note the very large *magnetic* intensities of over 2×10^4 counts/s obtained for this material on the bending-magnet beam line X22C at the NSLS. The approximate volume of the sample illuminated is $1\times0.5\times(1.2\times10^{-4})$ mm^3, taking a penetration depth of 1200 Å. This corresponds to 0.6×10^{-4} mm^3 or a mass of ~ 1 μg. The new generation synchrotron machines at Grenoble and Argonne will have a brightness at the undulator lines of some 10^3 times that the NSLS, allowing the same flux to be delivered into an area some 1000 times smaller. In the present case, this translates directly into a gain since the penetration will remain unchanged, so that, at least theoretically, we can foresee the possibility of examining transuranium samples of only 1 ng mass. Many questions, of course, remain unanswered. How to get single crystals? How to find them in the synchrotron beam? Nevertheless, projected investigations on actinide samples open up the possibility of magnetic studies in a region of the periodic table that is accessible, so far, only to superconducting quantum interference device (SQUID) magnetometers.[30]

ACKNOWLEDGMENTS

Our special thanks to Doon Gibbs who has aided us in all aspects of these experiments at the X22C beam line at the NSLS. We would like to express our thanks to the Special Materials and Radiation Protection group at BNL for helping us overcome the problems associated with using a Np-containing sample in the NSLS beam hall. Without their competence and cooperation, these experiments would not have been possible. We thank also Jane Brown, Paolo Carra, Denis McWhan, and Christian Vettier for discussions and J. C. Spirlet, C. Rijkeboer, and E. Bednarczyk for crystal growth and encapsulation. The high-purity Np metal required for the fabrication of this compound was made available through a loan agreement between Livermore National Laboratory and EITU, in the framework of a collaboration involving LLNL, Los Alamos National Laboratory, and the U.S. Department of Energy. S.L. and W.G.S. are grateful to the U.K. Science and Engineering Research Council for financial support. G.H.L. thanks the Physics Department, BNL, for partial support. Work performed at BNL was supported by the U.S. DOE under Contract No. DE-AC02-76CH00016.

[1]P. M. Platzmann and N. Tzoar, Phys. Rev. B **2**, 3556 (1970), M. Blume, J. Appl. Phys. **57**, 3615 (1985), and references therein.

[2]See, for example, D. Gibbs, Synchrotron Radiat. News **5**(5), 18 (1992); W. G. Stirling and G. H. Lander, *ibid.* **5**(4), 17 (1992); a comprehensive list of references is also given in G. H. Lander and W. G. Stirling, Phys. Scr. T **45**, 15 (1992).

[3]D. Gibbs, D. R. Harshman, E. D. Isaacs, D. B. McWhan, D. Mills, and C. Vettier, Phys. Rev. Lett. **61**, 1241 (1988); D. Gibbs, G. Grübel, D. R. Harshman, E. D. Isaacs, D. B. McWhan, D. Mills, and C. Vettier, Phys. Rev. B **43**, 5663 (1991).

[4]J. P. Hannon, G. T. Trammell, M. Blume, and D. Gibbs, Phys. Rev. Lett. **61**, 1245 (1988); **62**, 2644(E) (1989).

[5]G. Schütz, W. Wagner, W. Wilhelm, R. Zeller, R. Frahm, and G. Materlik, Phys. Rev. Lett. **58**, 737 (1987); **62**, 2620 (1989).

[6]B. T. Thole, G. van der Laan, and G. Sawatzky, Phys. Rev. Lett. **55**, 2086 (1985); B. T. Thole, P. Carra, F. Sette, and G. van der Laan, *ibid.* **68**, 1943 (1992).

[7]E. D. Isaacs, D. B. McWhan, C. Peters, G. E. Ice, D. P. Siddons, J. B. Hastings, C. Vettier, and O. Vogt, Phys. Rev. Lett. **62**, 1671 (1989); D. B. McWhan, C. Vettier, E. D. Isaacs, G. E. Ice, D. P. Siddons, J. B. Hastings, C. Peters, and O. Vogt, Phys. Rev. B **42**, 6007 (1990).

[8]E. D. Isaacs, D. B. McWhan, R. N. Kleiman, D. J. Bishop, G. E. Ice, P. Zschak, B. D. Gaulin, T. E. Mason, J. D. Garrett, and W. J. L. Buyers, Phys. Rev. Lett. **65**, 3185 (1990).

[9]J. A. Paixão, G. H. Lander, C. C. Tang, W. G. Stirling, A. Blaise, P. Burlet, P. J. Brown, and O. Vogt, Phys. Rev. B **47**, 8634 (1993).

[10]C. C. Tang, W. G. Stirling, G. H. Lander, D. Gibbs, W. Herzog, P. Carra, B. T. Thole, K. Mattenberger, and O. Vogt, Phys. Rev. B **46**, 5287 (1992).

[11]S. Langridge, W. G. Stirling, G. H. Lander, J. Rebizant, J. C. Spirlet, D. Gibbs, and O. Vogt, Europhys. Lett. **25**, 137 (1994).

[12]J. C. Spirlet and O. Vogt, in *Handbook on the Physics and Chemistry of the Actinides,* edited by A. J. Freeman and G. H. Lander (North-Holland, Amsterdam, 1984), Vol. 1, p. 79.

[13]See, for example, R. W. James, *The Optical Principles of the Diffraction of X-rays* (Bell, London, 1962), Chap. IV.

[14]G. Kalkowski, G. Kaindl, W. D. Brewer, and W. Krone, Phys. Rev. B **35**, 2667 (1987).

[15]P. Carra (private communication).

[16]A. T. Aldred, B. D. Dunlap, A. R. Harvey, D. J. Lam, G. H. Lander, and M. H. Mueller, Phys. Rev. B **9**, 3766 (1974).

[17]P. Burlet, D. Bonnisseau, S. Quezel, J. Rossaat-Mignod, J. C. Spirlet, J. Rebizant, and O. Vogt, J. Magn. Magn. Mater. **63-64**, 151 (1987).

[18]D. L. Jones, W. G. Stirling, G. H. Lander, J. Rebizant, J. C. Spirlet, M. Alba, and O. Vogt, J. Phys. Condens. Mater. **3**, 3551 (1991).

[19]D. L. Jones, S. Langridge, W. G. Stirling, G. H. Lander, J. Rebizant, J. C. Spirlet, M. Alba, and O. Vogt, Physica B **180-181**, 88 (1992).

[20]J. M. Fournier and E. Gratz, in *Handbook on the Physics and Chemistry of the Rare Earths,* edited by K. Gschneider, L. Eyring, G. H. Lander, and G. Choppin (North-Holland, Amsterdam, 1993), Vol. 17, Chap. 115.

[21]J. Rossat-Mignod, G. H. Lander, and P. Burlet, in *Handbook on the Physics and Chemistry of the Actinides,* edited by A. J. Freeman and G. H. Lander (North-Holland, Amsterdam, 1984), Vol. 1, p. 415.

[22]This can be compared to the peak intensity of a few hundred counts per second obtained at low temperature for the magnetic peaks with a single-crystal sample of 174 mg at the IN14 triple-axis spectrometer (pyrolytic graphite monochromator without analyzer) at the High-Flux Reactor of the Institute Laue Langevin, Grenoble, France. Furthermore, the resolution is a factor of ~ 5 better in the x-ray studies. The absorption of 4-Å neutrons in NpAs is 8 cm^{-1} (these comparisons are from Refs. 18 and 19).

[23]J. Luo, G. T. Trammell, and J. P. Hannon, Phys. Rev. Lett. **71**, 287 (1993).

[24]J. P. Hill, T. R. Thurston, R. W. Erwin, M. J. Ramsted, and R. J. Birgeneau, Phys. Rev. Lett. **66**, 3281 (1991).

[25]J. Bohr, D. Gibbs, J. D. Axe, D. E. Moncton, K. L. D'Amico, C. F. Majkrzak, J. Kwo, M. Hong, C. L. Chien, and J. Jensen, Physica B **159**, 93 (1989), and references therein; R. A. Cowley and S. Bates, J. Phys. C **21**, 4113 (1988); S. Bates, C. Patterson, G. J. McIntyre, S. B. Palmer, A. Mayer, R. A. Cowley, and R. Melville, *ibid.* **21**, 4125 (1988).

[26]P. J. Brown, S. M. Hayden, G. H. Lander, J. Zaretsky, C. Stassis, P. Metcalf, and J. M. Honig, Physica B **180-181**, 380 (1992).

[27]P. Burlet, S. Quezel, J. Rossat-Mignod, J. C. Spirlet, J. Rebizant, and O. Vogt, J. Magn. Magn. Mater. **63-64**, 145 (1987).

[28]H. W. Knott, G. H. Lander, M. H. Mueller, and O. Vogt, Phys. Rev. B **21**, 4159 (1980).

[29]J. G. Gay and R. Richter, Phys. Rev. Lett. **56**, 2728 (1986).

[30]P. G. Huray and S. E. Nave, in *Handbook on the Physics and Chemistry of the Actinides,* edited by A. J. Freeman and G. H. Lander (North-Holland, Amsterdam, 1987), Vol. 5, p. 311.